View metadata, citation and similar papers at core.ac.uk
brought to you by CORE
provided by University of Dayton

University of Dayton
eCommons

Chemical and Materials Engineering Faculty Publications | Department of Chemical and Materials Engineering

2004

Effect of Plasma Flux Composition on the Nitriding Rate of Stainless Steel

Christopher Muratore
University of Dayton, cmuratore1@udayton.edu

Scott G. Walton
Naval Research Laboratory

D. Leonhardt
Naval Research Laboratory

Richard F. Fernsler
Naval Research Laboratory

David D. Blackwell
Naval Research Laboratory

See next page for additional authors

Follow this and additional works at: https://ecommons.udayton.edu/cme_fac_pub

Part of the Other Chemical Engineering Commons, Other Materials Science and Engineering Commons, Petroleum Engineering Commons, Polymer and Organic Materials Commons, and the Thermodynamics Commons

eCommons Citation
Muratore, Christopher; Walton, Scott G.; Leonhardt, D.; Fernsler, Richard F.; Blackwell, David D.; and Meger, R. A., "Effect of Plasma Flux Composition on the Nitriding Rate of Stainless Steel" (2004). *Chemical and Materials Engineering Faculty Publications*. 112.
https://ecommons.udayton.edu/cme_fac_pub/112

This Article is brought to you for free and open access by the Department of Chemical and Materials Engineering at eCommons. It has been accepted for inclusion in Chemical and Materials Engineering Faculty Publications by an authorized administrator of eCommons. For more information, please contact frice1@udayton.edu, mschlangen1@udayton.edu.

Author(s)
Christopher Muratore, Scott G. Walton, D. Leonhardt, Richard F. Fernsler, David D. Blackwell, and R. A. Meger

This article is available at eCommons: https://ecommons.udayton.edu/cme_fac_pub/112

Effect of plasma flux composition on the nitriding rate of stainless steel

C. Muratore,[a] S. G. Walton, D. Leonhardt, R. F. Fernsler, D. D. Blackwell,[b] and R. A. Meger
Plasma Physics Division, Naval Research Laboratory Washington, DC 20375-5346

(Received 19 November 2003; accepted 29 March 2004; published 20 July 2004)

The total ion flux and nitriding rate for stainless steel specimens exposed to a modulated electron beam generated argon-nitrogen plasma were measured as a function of distance from the electron beam axis. The total ion flux decreased linearly with distance, but the nitriding rate increased under certain conditions, contrary to other ion flux/nitriding rate comparisons published in the literature. Variation in ion flux composition with distance was explored with a mass spectrometer and energy analyzer as a possible explanation for the anomalous nitriding rate response to ion flux magnitude. A transition in ion flux composition from mostly N_2^+ to predominantly N^+ ions with increasing distance was observed. Significant differences in molecular and atomic nitrogen ion energy distributions at a negatively biased electrode were also measured. An explanation for nitriding rate dependence based on flux composition and magnitude is proposed. [DOI: 10.1116/1.1752894]

I. INTRODUCTION

Nitriding refers to any surface modification process that increases the local concentration of nitrogen in a material. Many metals and alloys have shown increased hardness and wear resistance resulting from incorporation of 5 to 50 atomic percent nitrogen.[1,2] Austenitic stainless steel is a particularly good candidate for nitriding, since it is soft compared to other engineering materials but is often found in applications in which wear resistance would be beneficial.[3] Unfortunately, austenitic stainless steel is a difficult material to nitride thermally because processing temperatures below 450 °C are required to maintain the corrosion resistance of most useful alloys[4] and such low temperatures inhibit nitrogen diffusion, which is the physical basis for the process. Additionally, the presence of stable chromium oxide compounds readily formed at a stainless steel surface inhibit nitrogen diffusion,[5] resulting in very slow nitride layer growth. Because of these complicating factors, plasma assisted diffusion-based techniques are usually employed for stainless steel nitriding. The plasma serves to deliver chemically reactive nitrogen species to the substrate surface, thereby resulting in higher nitriding rates at lower temperatures. In these processes, the rate and nitrided layer properties correlate to the characteristics of the plasma. For example, it has been shown that the nitride growth rate under low energy (<1000 eV) ion bombardment is linearly proportional to the magnitude of the N_2^+ ion flux.[6,7] This rate dependence is attributed to two processes that are enhanced with increasing ion flux: (1) nitrogen diffusion due to an increased supply of N atoms resulting from impact dissociation of molecular nitrogen ions[6,8] and (2) rapid oxide layer removal by sputtering.[5,8]

The current work describes experiments in a modulated electron beam generated plasma nitriding system[9] in which samples of AISI 316 stainless steel showed a nonlinear response to the total ion flux, where, under certain conditions, the nitriding rate increased with decreasing ion flux. To better understand the observed nitriding rate dependence on the magnitude of the ion flux, a mass spectrometer and energy analyzer were used to examine the composition of the plasma flux. The results suggest that the nitriding rate is dependent not only upon the magnitude, but also upon the composition of the flux from the plasma.

II. EXPERIMENT

Figure 1 illustrates the reaction chamber fitted with an electrically isolated 11 cm diameter sample stage mounted on a linear motion feedthrough. The stage consisted of a 0.15 cm thick, 11 cm diameter stainless steel disk backed by an 11.5 cm diameter disk of boron nitride which housed a resistive heating element. Samples of 0.15 cm thick electropolished AISI 316 stainless steel with a surface area of 6.5 cm^2 were secured to the front of the stage, and the system was pumped down to a base pressure of 1×10^{-4} Pa. The chamber pressure was then increased to 21.3 Pa, with 87.5% nitrogen and 12.5% argon. The samples were heated to 415 °C (±3 °C) in 30 min, and maintained at that temperature for an additional 6.5 h while dc biased to -350 V and exposed to the electron beam generated plasma. The electron beam was produced by a pulsed hollow cathode operated at -2 kV and modulated at 500 Hz and 50% duty factor. The beam was confined by an axial magnetic field of approximately 150 G, generated by a pair of Helmholtz coils located outside the chamber. The hollow region of the cathode measured 15 cm$\times$1 cm and was 1 cm deep. The electron beam emitted from the hollow region passed through a 15 cm$\times$1 cm wide slot in a grounded plate (slotted anode) and terminated at an anode located 60 cm from the slotted anode. The cross sectional area of the beam was defined by both the hollow cathode geometry and the slotted anode, and was maintained over the beam length by the magnetic field. The exposure time (50% of 7 h) of the substrate to the active phase of plasma production was used to calculate the nitriding rates,

[a] ASEE/NRL Postdoctoral Research Fellow; electronic mail: cmurator@ccs.nrl.navy.mil
[b] SFA Inc., Largo, MD 20744.

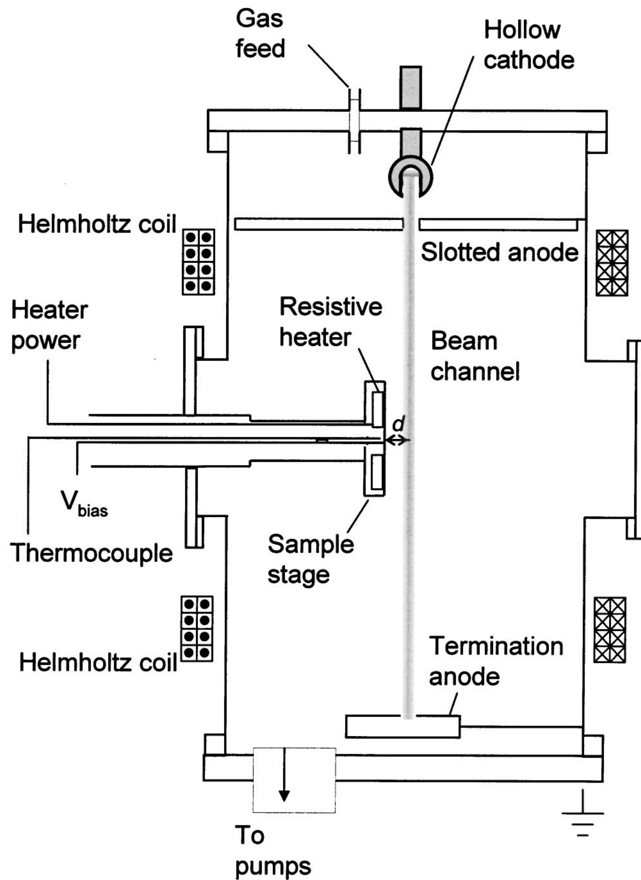

FIG. 1. Schematic of the processing chamber. Note that d indicates the distance from the substrate to the electron beam axis.

which were determined by assuming diffusion controlled growth at a rate proportional to the square root of time ($t^{1/2}$).[9,10] The samples were nitrided under identical conditions at 0.5 cm increments starting at position $d=1.5$ cm (where $d=0$ is defined as the center of the beam channel) to $d=4.0$ cm. After nitriding, the specimens were sputter coated with metal while maintained at room temperature and sectioned. The cross-sections were polished and etched in acid to allow observation of the nitrided layer thickness in an optical microscope. The thickness was measured with the cursors of a Vickers microindentor with 0.2 μm resolution.

The total ion flux was determined by measuring the current to the sample stage during the nitriding experiments.

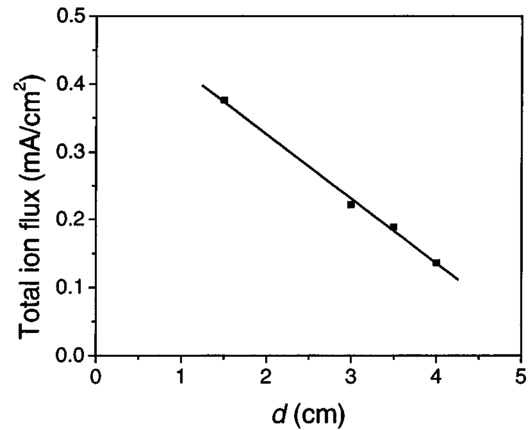

FIG. 2. Total positive ion flux incident on the heated and biased substrate exhibits a linear dependence on the distance from the electron beam axis d.

Since the stage area was very large compared to the sheath thickness (s), the current measurements were independent of s.[12] Additionally, the probability of secondary electron emission from stainless steel at the ion energy employed was on the order of 0.1,[13] and was not considered when reporting the ion flux.

A magnetically shielded Hiden Analytical electrostatic quadrupole plasma (EQP) analyzer was used to measure the temporally resolved ion energy distributions and relative flux of each specie at a grounded electrode in a separate but similar vacuum chamber described elsewhere.[11] With the exception of substrate bias, plasmas were generated under similar conditions as those used in the nitriding experiments. The positive ion flux measured at the sample stage during the nitriding experiments was assumed to be comprised of the same relative flux of ions as that measured with the EQP analyzer at each distance d.

To measure N_2^+ and N^+ ion energy distributions at a biased electrode, a 100 V dc bias was applied to the termination anode. This voltage raised the plasma potential by 100 V, and created a sheath with an approximate -100 V potential drop to the grounded EQP front electrode.[14]

III. RESULTS

Figure 2 shows the integrated total ion flux averaged over 200 periods of cathode operation at the biased substrate stage located at the indicated position relative to the electron beam

TABLE I. Nitride layer thickness, total ion flux, and contribution of each ion specie to the total flux at each position relative to the electron beam axis.

d (cm)	Nitride layer thickness (μm)	Total ion flux (ions cm^{-2} s^{-1})	N_2^+ ion flux (ions cm^{-2} s^{-1})	N^+ ion flux (ions cm^{-2} s^{-1})	Ar^+ ion flux (ions cm^{-2} s^{-1})
1.5	6.7	2.4×10^{15}	1.3×10^{15}	9.2×10^{14}	1.6×10^{14}
2.0	2.8	2.1×10^{15}	1.0×10^{15}	8.8×10^{14}	1.0×10^{14}
2.5	1.3	1.8×10^{15}	8.4×10^{14}	8.2×10^{14}	8.8×10^{13}
3.0	1.9	1.5×10^{15}	6.1×10^{14}	7.8×10^{14}	5.8×10^{13}
3.5	1.9	1.2×10^{15}	3.8×10^{14}	7.4×10^{14}	3.5×10^{13}
4.0	1.1	8.5×10^{14}	1.8×10^{14}	6.6×10^{14}	1.7×10^{13}

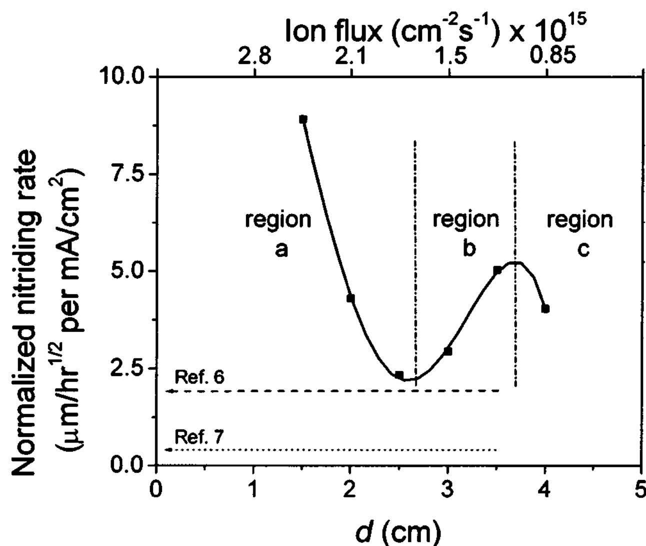

FIG. 3. Nitriding rate at different values of d and normalized by the magnitude of the total ion flux for the electron beam generated plasma. Also shown are normalized nitriding rates from Refs. 6 and 7. The top scale shows how the ion flux changed with distance in the electron beam generated system, and does not correlate to the referenced data.

axis. The flux decreased linearly with increasing distance. Table I contains the ion flux data plotted in Fig. 2 and the nitride layer thickness measured after processing. Figure 3 shows the nitriding rate normalized to the total ion flux. The nitriding rate (whether normalized or not) exhibits two maxima when plotted against distance, one close to the electron beam ($d = 1.5$ cm) and a second at $d = 3 - 4$ cm, even though the ion flux decreased monotonically with d over this range. Also shown in Fig. 3 are normalized nitriding rates taken from Williamson *et al.*[6] and Brokman *et al.*[7] Note that in Ref. 6 the ion flux was reported to be predominantly N_2^+, and in Ref. 7 the flux was comprised of an unknown mixture of nitrogen and hydrogen ions. In both works the ion flux composition did not vary and the nitriding rate was proportional to the ion flux, and is therefore constant after normalization. Although the total ion flux was lower in the electron beam generated plasma, the nitriding rate is high compared to the referenced works, and other nitriding processes at similar temperatures.[9]

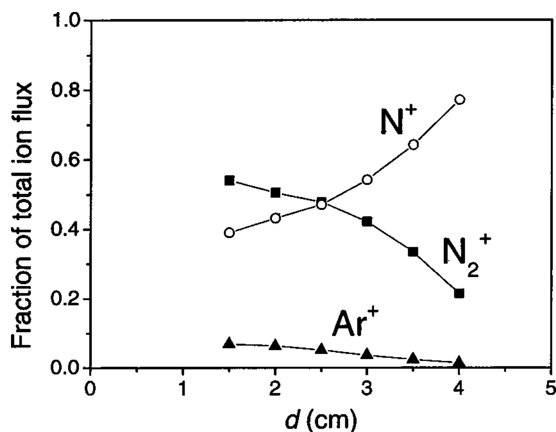

FIG. 4. Relative N_2^+, N^+, and Ar^+ fluxes for different values of d.

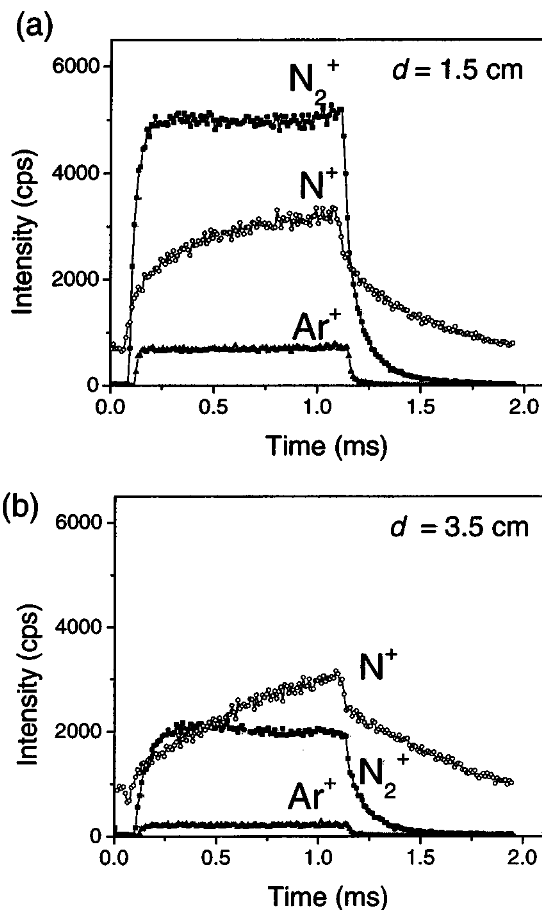

FIG. 5. Time-resolved flux of each of the three dominant ion species incident on a grounded electrode placed at (a) $d = 1.5$ cm and (b) $d = 3.5$ cm over one period of cathode operation.

Figure 4 shows for each distance d the contribution of each ion specie to the total ion flux over an entire cathode period measured with the EQP analyzer. The flux was composed of predominantly N_2^+ ions between $d = 1.5$ and 2.5 cm, while at greater distances most of the flux consisted of N^+ ions. Table I lists quantitative fluxes of N_2^+, N^+, and Ar^+ ions, estimated by relating the relative flux as shown in Fig. 4 to the total flux plotted in Fig. 2. The argon ion flux never exceeded 7% of the total flux. Figure 5 shows the time-resolved flux (a) at $d = 1.5$ cm and (b) $d = 3.5$ cm for each of the three ion species. In both figures, the flux of N_2^+ ions decayed much more rapidly than the N^+ ion flux in the plasma afterglow. Additionally, the N_2^+ flux decreased significantly as d increased, but the N^+ ion flux was comparable at both distances.

Figure 6 shows N_2^+ and N^+ ion energy distributions collected only during the beam pulse and normalized to their respective areas. The grounded EQP electrode was located at $d = 1.5$ cm in the electron beam generated plasma, which was biased to +100 V. The atomic nitrogen ions exhibited energy distributions that corresponded well to the sheath potential of

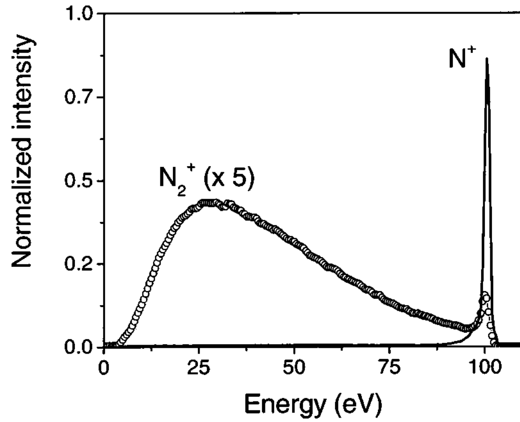

FIG. 6. Normalized ion energy distributions for molecular and atomic nitrogen ions incident on an electrode located at $d = 1.5$ cm and biased to approximately -100 V relative to the plasma.

100 V, but the molecular ions displayed significantly lower energies, with a most probable energy of approximately 25 eV.

IV. DISCUSSION

Figure 3 shows that the nitriding rate varied nonlinearly with the total ion flux. Since the dependence is known to be linear when the flux composition is constant, it can be presumed that the nitriding rate depended on the composition as well as the magnitude of the ion flux to the substrate in the electron beam system. To further understand this dependence, it is necessary to understand the mechanisms by which the magnitude and energy distributions of the ion fluxes changed with time and distance from the plasma source, and to consider a qualitative flux balance based on the data from the mass spectrometer.

The rapid decay of N_2^+ and Ar^+ compared to N^+ in the afterglow, as observed in Fig. 5 can be explained by considering the dominant loss mechanisms of each ion. The time to diffuse to the chamber walls determines the lifetime of the N^+ ions, which have no other competitive loss mechanism. This diffusion time has been shown to be on the order of milliseconds for this system[11] under similar conditions. For the argon ions, decay is dominated by charge exchange with nitrogen molecules with a rate constant $k_{ce} \sim 10^{-11}\,\mathrm{cm^3\,s^{-1}}$ (Ref. 15). Their destruction time is given by

$$\tau_{ce} = (k_{ce} n_g)^{-1} \approx 20\ \mu\mathrm{s}$$

for the background nitrogen gas density $n_g \approx 5 \times 10^{15}\,\mathrm{cm^{-3}}$. Finally, the molecular nitrogen ion recombines rapidly with electrons in the reaction

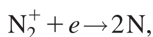

$$N_2^+ + e \rightarrow 2N,$$

and is destroyed in a time given by

$$\tau_r = (\beta n_e)^{-1} \approx 100\ \mu\mathrm{s},$$

where the dissociative recombination coefficient, $\beta \sim 10^{-7}\,\mathrm{cm^3\,s^{-1}}$ (Ref. 16), and the electron density, $n_e \approx 10^{11}\,\mathrm{cm^3}$ (Ref. 17).

TABLE II. Calculated values of N atom flux at each distance from the beam axis d. The flux at $d = 1.5$ cm was assumed to be only that generated directly by the beam electrons.

d (cm)	N atom flux (atoms $\mathrm{cm^{-2}\,s^{-1}}$)
1.5	1.0×10^{14}
2.0	7.0×10^{14}
2.5	1.0×10^{15}
3.0	1.5×10^{15}
3.5	1.9×10^{15}
4.0	2.3×10^{15}

Therefore, the flux of molecular ions is reduced more rapidly than the flux of atomic nitrogen ions due to electron-ion recombination. In Fig. 5, where N_2^+ and Ar^+ ions are shown to have decayed rapidly with time compared to N^+ ions, the decay times in the afterglow were comparable to the above calculations. The rapid destruction of N_2^+ ions through dissociative recombination similarly leads to the spatial dependence observed in Fig. 4, where N^+ is the most abundant ion for $d > 2.5$ cm.

As the molecular nitrogen ions were lost to the dissociative recombination reaction, the local N atom flux to the substrate was increased with distance from the beam. The magnitude of the increase can be estimated by the difference of the N_2^+ ion flux at $d = 1.5$ cm, to that measured further from the beam axis. For example, Table I lists the N_2^+ ion flux at $d = 3.5$ cm as $3.8 \times 10^{14}\,\mathrm{ions\,cm^{-2}\,s^{-1}}$ compared to 1.3×10^{15} at 1.5 cm. If all of the N_2^+ ions lost in traversing the 2 cm distance were converted to N atoms, the local N flux would have increased by about $1.8 \times 10^{15}\,\mathrm{cm^{-2}\,s^{-1}}$. This is significantly larger than the flux of N atoms generated directly by the electron beam, which is estimated to be one tenth of the ion flux based on the pertinent cross sections,[18] or approximately $1 \times 10^{14}\,\mathrm{cm^{-2}\,s^{-1}}$. Values of atomic nitrogen flux were calculated in this way for all values of d in Table II. The nitriding rate of stainless steel is strongly dependent on the magnitude of the flux of N atoms in plasma assisted nitriding processes.[19–21] For larger values of d, the magnitude of the calculated N atom flux is on the same order as the concentration of nitrogen retained in the nitrided metal, and is therefore of sufficient magnitude to affect the process.

Another factor that may have contributed to the observed nitriding response to ion flux is the effect of charge exchange on the ion energy distributions at a biased electrode. Figure 6 shows that few of the N_2^+ ions arrived with kinetic energy equivalent to the full sheath potential, while nearly all of the N^+ ions impacted the surface with an energy near that of the applied bias at $d = 1.5$ cm. The molecular ions most likely lost their energy in the reaction

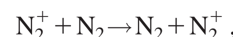

$$N_2^+ + N_2 \rightarrow N_2 + N_2^+,$$

due to the large resonant charge exchange cross section $Q_{ce} \approx 3.1 \times 10^{-15}\,\mathrm{cm^2}$ at 100 eV.[22] The ion mean free path for molecular charge exchange collisions (λ_{ce}) is given by

$$\lambda_{ce} \approx (Q_{ce} n_g)^{-1} \approx 0.05 \text{ cm},$$

where n_g is the nitrogen gas number density. By contrast, the atomic nitrogen ions mainly suffer elastic collisions with N_2 molecules, with a momentum transfer cross section $Q_m \approx 2.9 \times 10^{-16}\,\text{cm}^2$.[22] The momentum transfer mean free path is thus given by

$$\lambda_m \approx (Q_m n_g)^{-1} \approx 1 \text{ cm}.$$

The sheath width (s) is related to the sheath potential $V_s = 100\,\text{V}$, and ion density at the sheath edge $n_s \approx 10^{10}$ by

$$s \approx 740[2V_s/n_s]^{1/2} \approx 0.1 \text{ cm},$$

as derived in Lieberman and Lichtenberg,[12] which provides a reasonable estimate for s in a weak, transverse magnetic field.[23] The sheath width is twice the charge exchange mean free path of the N_2^+ ions, but shorter than the N^+ ion momentum transfer mean free path. Thus, the molecular ions were likely to collide within the sheath, while the atomic ions were not. The atomic ions therefore arrived at the substrate with the full sheath potential, while the molecular ions arrived over a range of much lower energies, as seen in Fig. 6. The current diagnostic hardware configuration would not allow measurements of ion energy distributions for sheath potentials greater than 100 V, however, the 350 V bias condition used for the nitriding experiments would double the sheath thickness and result in an even greater reduction in the N_2^+ ion energy. Furthermore, the total ion flux, which is linearly proportional to the plasma density at the sheath edge,[24] was shown to decrease with increasing distance in Fig. 2, suggesting an expanding sheath width and therefore a more pronounced decrease in the most probable molecular ion energy with increased d.

The observed reduction in N_2^+ ion energy is significant for two reasons. As indicated previously, sputtering of the substrate during nitriding is necessary in low energy, high vacuum processes to prevent surface oxide formation, which has been shown to inhibit nitride layer growth.[5,25] Transport of Ions in Matter (TRIM) simulations show that the sputter yield of oxygen in iron by low energy (<100 eV) molecular nitrogen ions is at least two orders of magnitude lower than the yield for the atomic ion at 350 eV therefore, the contribution of N_2^+ ions toward surface sputtering is minimal. Additionally, the adsorption probability of N_2^+ decreases with decreasing ion energy,[26] limiting the ability of the molecular ion to increase the concentration of nitrogen at the substrate surface.

Based on the analysis of the flux presented above, the authors postulate that the normalized nitriding rate dependence on the total ion flux shown in Fig. 3 can be attributed to both the magnitude and composition of the flux of plasma species to the substrate. In the region a in Fig. 3, the concentration of N atoms on the surface resulting from impact dissociation of energetic molecular ions and adsorption of the N^+ ions was greater than the flux of N atoms generated in the plasma (j_N). Under these conditions (similar to those in Refs. 6 and 7), the surface concentration of N atoms, and thus the nitriding rate, directly corresponded to the total ion flux (j_i). Comparison of the quantitative ion flux data in Table I compared to the N fluxes in Table II support this argument. Region b in Fig. 3 shows an increase in nitriding rate with a decrease in ion flux. In this region, it is proposed that the flux of N atoms produced in the plasma, particularly by decay of N_2^+ ions, was greater than that generated on the surface via dissociation of energetic N_2^+ ions and from the N^+ ion flux. Additionally, the plasma sheath broadened with decreasing plasma density. The increased sheath width likely reduced the most probable N_2^+ ion energy from 25 eV at $d = 1.5\,\text{cm}$, and thereby decreased the number of incident N_2^+ ions contributing to the concentration of N at the substrate. The ion flux and energy in region b, although smaller, were nevertheless sufficient to maintain an oxide free substrate surface, which was subjected to an oxygen flux (j_O) of approximately 1×10^{14} oxygen atoms $\text{cm}^{-2}\,\text{s}^{-1}$ based on kinetic theory and the system base pressure. In region c, the N flux increased with d, but the oxygen sputter rate (S_O) was no longer sufficient to maintain an oxide free substrate due to the reduced magnitude and energy of the ion flux, and the nitriding rate decreased. To summarize, the nitriding rate appears to be controlled by j_i when $j_i > j_N$, and dictated by j_N when $j_i < j_N$, provided $S_O > j_O$.

V. CONCLUSION

Stainless steel specimens were subjected to a variable ion flux in a modulated electron beam generated argon-nitrogen plasma system by incrementally increasing the distance of the substrate from the electron beam axis. The observed nitriding rates did not scale in proportion to the total ion flux as in the work of others, where the ion flux composition was held constant. Ion flux characterization experiments were also performed under similar conditions to measure temporal and spatial flux composition. Mass spectrometry showed a significant decrease in the N_2^+ ion flux with increasing d, but a constant atomic nitrogen ion flux for all values of d, and also suggested a significant increase in neutral atomic nitrogen flux with increasing distance. Mass-resolved ion energy distributions showed that atomic nitrogen ions exhibited an energy commensurate with the sheath voltage, while a majority of the N_2^+ ions did not. The results indicate that the nitriding rate of stainless steel depends on both the magnitude and composition of the ion flux.

The dependence of nitriding rate on flux composition suggests that an ideal stainless steel nitriding environment would include a moderate energetic ion flux, sufficient to sputter surface oxides but with minimal alteration of workpiece surface finish by excess heating or sputtering, and a large neutral flux to enhance nitrogen diffusion in the substrate. One means of achieving these conditions is to employ a source that generates a large atomic ion flux. Such a system can be employed at higher pressures to increase the neutral flux without the loss of ion energy due to charge exchange reactions in the plasma sheath. The electron beam generated plasma system employed in this work demonstrates these characteristics, and has exhibited high nitriding rates com-

pared to other plasma assisted nitriding systems which typically exhibit higher ion fluxes.

ACKNOWLEDGMENTS

This research was supported by the Office of Naval Research. C.M. appreciates the support of the American Society for Engineering Education.

[1] D. L. Williamson, J. A. Davis, and P. J. Wilbur, Surf. Coat. Technol. **103–104**, 178 (1998).
[2] H. R. Stock, C. Jarms, F. Seidel, and J. E. Döring, Surf. Coat. Technol. **94–95**, 247 (1997).
[3] T. Czerwiec, N. Renevier, and H. Michel, Surf. Coat. Technol. **131**, 267 (2000).
[4] Z. L. Zhang and T. Bell, Surf. Eng. **1**, 131 (1985).
[5] S. Parascandola, O. Kruse, E. Richter, and W. Moeller, J. Vac. Sci. Technol. B **17**, 855 (1999).
[6] D. L. Williamson, J. A. Davis, P. J. Wilbur, J. J. Vajo, R. Wei, and J. N. Matossian, Nucl. Instrum. Methods Phys. Res. B **127/128**, 930 (1997).
[7] A. Brokman and F. R. Tuler, J. Appl. Phys. **52**, 468 (1981); [note that the original data in the paper was replotted by the current authors to see the linear flux/nitriding rate dependence and the fluxes were higher (>10 mA cm^{-2}) than those studied here].
[8] R. Wei, Surf. Coat. Technol. **83**, 218 (1996).
[9] C. Muratore, D. Leonhardt, S. G. Walton, D. D. Blackwell, R. F. Fernsler, and R. A. Meger, Surf. Coat. Technol. (to be published).
[10] D. L. Williamson, O. Ozturk, R. Wei, and P. J. Wilbur, Surf. Coat. Technol. **65**, 15 (1994).
[11] S. G. Walton, D. Leonhardt, D. D. Blackwell, R. F. Fernsler, D. P. Murphy, and R. A. Meger, Phys. Rev. E **65**, 046 412 (2002).
[12] M. A. Lieberman and A. J. Lichtenberg, *Principles of Plasma Discharges and Materials Processing* (Wiley, New York, 1994).
[13] J. R. McNeil, J. J. McNally, and P. D. Reader, in *Handbook of Thin-Film Deposition Processes and Techniques*, edited by K. Seshan (Noyes, Park Ridge, NJ, 2002).
[14] J. W. Coburn and E. Kay, J. Appl. Phys. **43**, 4965 (1972).
[15] Y. Ikezoe, S. Matsuoka, M. Takebe, and A. Viggiano, *Gas Phase Ion-Molecule Reaction Rate Constants Through 1986* (Mass Spectroscopy Society of Japan, Tokyo, 1987).
[16] F. J. Mehr and M. A. Biondi, Phys. Rev. **181**, 264 (1969).
[17] D. Leonhardt, S. G. Walton, D. D. Blackwell, W. E. Amatucci, D. P. Murphy, R. F. Fernsler, and R. A. Meger, J. Vac. Sci. Technol. A **19**, 1367 (2001).
[18] P. C. Cosby, J. Chem. Phys. **98**, 9544 (1993).
[19] G. C. Tibbetts, J. Appl. Phys. **45**, 5072 (1974).
[20] G. Henrion, R. Hugon, M. Fabry, and V. Scherentz, Surf. Coat. Technol. **97**, 729 (1997).
[21] M. J. Baldwin, S. C. Haydon, and M. P. Fewell, Surf. Coat. Technol. **97**, 97 (1997).
[22] A. V. Phelps, J. Phys. Chem. Ref. Data **20**, 557 (1991).
[23] K.-U. Reimann, Phys. Plasmas **1**, 552 (1994).
[24] D. M. Manos and H. F. Dylla, in *Plasma Etching: An Introduction*, edited by D. M. Manos and D. L. Flamm (Academic, San Diego, 1989).
[25] M. P. Fewell, J. M. Priest, M. J. Baldwin, G. A. Collins, and K. T. Short, Surf. Coat. Technol. **131**, 284 (2000).
[26] H. F. Winters, D. E. Horne, and E. E. Donaldson, J. Chem. Phys. **41**, 2766 (1964).